J. Phys.: Condens. Matter **11** (1999) 5929–5952. Printed in the UK PII: S0953-8984(99)01386-7

# Spin relaxation in low-dimensional systems

L Viña

Departamento de Física de Materiales C-IV-510, Universidad Autónoma de Madrid, Cantoblanco, E-28049 Madrid, Spain

E-mail: luis.vina@uam.es

Received 28 January 1999

**Abstract.** We review some of the newest findings on the spin dynamics of carriers and excitons in GaAs/GaAlAs quantum wells. For intrinsic wells, whose optical properties are dominated by excitonic effects, we show that exciton–exciton interaction produces a breaking of the spin degeneracy in two-dimensional semiconductors. For doped wells, the two spin components of an optically created two-dimensional electron gas are well described by Fermi–Dirac distributions with a common temperature but different chemical potentials. The rate of the spin depolarization of the electron gas is found to be independent of the mean electron kinetic energy but accelerated by thermal spreading of the carriers.

## 1. Introduction

Useful electronic devices rely on the precise control of electronic charge, and, in general, the fact that the electrons also have a spin is ignored. However, the scattering processes for electrons depend on their spin state. Spin-related effects of carriers are attracting a lot of attention in different fields of condensed matter physics. Recently, interest in electronic spin polarization in solid-state systems has grown, fuelled by the possibility of producing efficient photoemitters with a high degree of polarization of the electron beam, creating spin-memory devices and spin transistors as well as exploiting the properties of spin coherence for quantum computation. The determination of the spin-flip rates is extremely important for electronic applications, because if the spins relax too rapidly, the distances travelled by spin-polarized currents will be too short for practical applications.

Studies on spin-polarized transport are growing dramatically in number, especially for ferromagnetic metals, which exhibit a splitting between the up- and down-spin states (‘exchange splitting’) to lower the total energy of the system by avoiding the high energy required to have a high density of states at the Fermi level. Therefore the current-carrying electrons at the Fermi level should be polarized. However, in experiments on tunnelling from a ferromagnetic metal film through a non-magnetic insulating barrier into a superconducting metal film, it was found, surprisingly, that the percentage polarization of the current scaled with the total magnetic moment, given by the net polarization of the electrons, and not with the polarization of the electrons at the Fermi level [1].

Devices such as a magnetic valve, which exploits the dependence of spin-polarized transport upon the spin-dependent density of states available at the Fermi level in two ferromagnetic metal films, have been demonstrated. These devices are analogous to optical polarizers; however, the minimum transport is obtained when the magnetic moments of the

0953-8984/99/315929+24$30.00  

two magnetic films are rotated by 180$^\circ$ away from the parallel, whereas for the optical case the minimum transmission is obtained for 90$^\circ$ orientation of the polarizer axis [1]. Very recently, Monsma *et al* have established that spin-dependent scattering of electrons can be exploited in a metal-base transistor-like structure [2]. This can be obtained by launching hot electrons from a semiconductor emitter into a very thin metallic magnetic base. As for optical devices, an all-optical gate switch, which uses the polarization-dependent optical non-linearity of 2D excitons in quantum wells (QWs), has been proposed and high-speed picosecond switching has been demonstrated [3]. Photon-spin-controlled lasing oscillations in GaAs surface-emitting lasers at room temperature have also been reported very recently [4].

There are various experiments that one can carry out to detect optical orientation, such as investigations of the spin polarization of the electron photoemission, electron paramagnetic resonance, nuclear magnetic resonance, spin-dependent transport, and Faraday rotation, and also making spin-dependent pump-and-probe or recombination measurements. The Hanle effect [5], i.e., the spin depolarization of carriers subject to a transverse magnetic field, has been traditionally used to obtain quantitative values for the spin-relaxation times [6–8]. Optical pumping, with linearly polarized light, and orientation, with circularly polarized light, of carrier spins are powerful methods for investigating relaxation processes in semiconductors, and have also found applications in spin-polarized electron sources. With the appearance of ultrafast lasers, the spin-relaxation time can also be measured in a direct way. Ultrafast time-resolved photoluminescence (TR-PL) has proven to be a very useful tool for probing the carrier dynamics in semiconductors. The emitted luminescence, after excitation with a light pulse, reflects the temporal evolution of the carrier distribution, and can be analysed to study the energy as well as the orientation-relaxation rates [9].

For bulk semiconductors, the spin relaxation of excitons and free carriers has been extensively studied in the past [9–12]. Most of the investigations have dealt with the study of conduction band electrons in p-type materials [13–18], or excitons in intrinsic ones [19–21]. A polarization analysis of the band-to-band luminescence was performed to obtain the various energy, momentum and spin-relaxation mechanisms for electrons [22, 23]. The amount of work has been more limited on n-type materials [7, 8, 24–26]. The experimental work was stimulated by theoretical studies of spin-relaxation processes by Elliot and Yafet [27, 28], D'yakonov and Perel' (DP) [29–31] and Bir *et al* [32], and different mechanisms responsible for the spin-flip processes have been identified [9, 15, 17, 33, 34]. The dependence of the various spin-relaxation mechanisms on temperature and doping has been used to distinguish between them [35–37].

The relative importance of these mechanisms is modified in semiconductor QWs mainly for three reasons:

(a) the new electronic bandstructure, which affects the hole spin relaxation;
(b) the enhancement of the excitonic effects, leading to a larger spin-flip rate due to exciton exchange; and
(c) the higher carrier mobility, which is important for mechanisms sensitive to carrier momentum relaxation, such as the DP one [29].

Experimental investigations on the spin dynamics in low-dimensional semiconductors have flourished in the last decade. Many studies deal with the spin processes of excitons [38–60], including indirect excitons in type II QWs [61], excitons in zero-dimensional quantum discs [62], the influence of external electric fields [63], and the inhibition of spin relaxation by a fast energy-relaxation process (emission of a longitudinal optical phonon) [64]. Fewer investigations deal with the spin flips of individual electrons and holes in 2D systems [45, 48, 65–71]. Extensive theoretical studies have also been made of the spin-flip relaxation of free carriers, electrons and holes [72–79], and excitons [80–87] in low-dimensional systems.

In quasi-two-dimensional systems the exciton energy is renormalized to higher values at high densities [88, 89]. A model given by Schmitt-Rink *et al* predicted that this effect would occur as a consequence of a strong reduction of the long-ranged Coulomb correlation interaction in a 2D system [90]. This is in strong contrast with the situation for three-dimensional excitons, which maintain their energies even at high densities. This effect is due to a compensation between two many-body effects: a repulsive contribution originating in the Pauli exclusion principle acting on the fermions forming the excitons, and an attractive one, similar to a van der Waals interaction. The latter is precisely reduced in 2D systems giving rise to the blue-shift of the excitons with increasing density.

An additional effect has been observed when a dense gas of excitons with a well defined spin is created [45]. Using circularly polarized ($\sigma^+$) light to excite the samples, close to the resonant formation of heavy-hole (hh) excitons, an energy splitting between the two components, $\sigma^+$ and $\sigma^-$, of the hh exciton luminescence has been reported. The $\sigma^+$ component is always at higher energies than that of $\sigma^-$ helicity. This effect has also been confirmed by other TR-PL studies [51, 70, 91–93] and by femtosecond pump-and-probe measurements for GaAs QWs under an external magnetic field [94]. A model has recently been developed which explains it as arising from inter-excitonic exchange interaction [95, 96].

Some other manifestations of spin-dependent exciton–exciton interactions have also been seen recently [57, 70]. They include a spin-dependent optical dephasing time and a linewidth difference between the two photoluminescence components $\sigma^+$ and $\sigma^-$ (the luminescence component co-polarized with the laser excitation is narrower than the counter-polarized one). All of these features can be interpreted as results of inter-excitonic exchange.

Exciton, as well as individual electron and hole, spin dynamics have also been investigated, in the presence of an external magnetic field, for heterostructures based on diluted semimagnetic semiconductors such as $Zn_{1-x}Mn_xSe$, using ultrafast Faraday spectroscopy [97–100] and TR-PL [101], or $Cd_{1-x}Mn_xTe$ [102]. A very rich variety of spin phenomena, absent in traditional semiconductor heterostructures, have been found in the Faraday rotation experiments, and the important role played by the effects of the correlation between excitons of different spin has been recognized [103]. Some of the results of these experiments seem to be sample dependent: while for the $Cd_{1-x}Mn_xTe$ system it has been found that spin-flip scattering times are independent of the strong spin–spin exchange interaction between the carriers and the magnetic ions, in strong contrast with calculations which show that the s–d exchange is a very efficient spin-flip scatterer for electrons in these systems [75], for the $Zn_{1-x}Mn_xSe$ system [101] the experiments are in agreement with the theoretical predictions. Time-resolved Kerr reflectivity experiments on modulation-doped $Zn_{1-x}Cd_xSe$ QWs have shown that the electron spin polarization, at low temperatures, lasts nearly three orders of magnitude longer than in insulating samples [104, 105]. For the same system, but undoped, pump–probe and degenerate four-wave-mixing experiments have manifested that the decay of exciton spin, after resonant excitation, occurs in a time shorter than the exciton dephasing time, and this effect has been attributed to alloy disorder [60].

Kuzma *et al* have studied the spin polarization of a two-dimensional electron gas (2DEG) buried within a semiconductor heterostructure in the fractional quantum Hall regime [71]. Using a site-selective nuclear magnetic resonance technique they have discovered several unexpected properties of this system when the occupation of electrons is in the fractional quantum Hall limit, with $\nu = 1/3$. Their data demonstrate that the spin polarization of the 2DEG decreases as the system is tuned away from $\nu = 1/3$, revealing the presence of spin-reversal charged excitations. These findings suggest a remarkable decoupling between the energy of the 2DEG spins and their environment. This is an important point for the fabrication of spin-polarized devices. A second important feature is the ability to manipulate the spin system, and Kuzma *et al* have also shown that radio-frequency radiation couples to these spin excitations. This suggests the exciting possibility that resonance techniques conventionally targeted at nuclear spins may ultimately prevail in controlling these electronic spins as well.

The studies of the dynamics of the coherent control of excitons [106–110], which provide a deep insight into interaction processes of excited states, have also been used to investigate the optical orientation of excitons in $Zn_{1-x}Mn_xSe$ [97–100] and GaAs QWs [57, 70, 111–114]. In the work of the Toulouse group [112], the optical dephasing time of excitons, their longitudinal and transverse spin-relaxation times, and their radiative lifetimes, are measured under the same experimental conditions, on the basis of the linear response of the samples.

In this work, we will focus primarily on time-resolved polarized photoluminescence. The rest of the article is organized as follows. Section 2 gives the experimental details. The spin-flip processes in intrinsic QWs are presented in section 3.1. The splitting between polarized excitons is shown in section 3.2. Section 3.3 introduces the spin decay and population distribution of an optically pumped 2DEG. The temperature dependence of the electron spin-flip times is given in section 3.4. Finally, we summarize in section 4.

## 2. Experimental details

The time-resolved experiments were performed in a variable-temperature, cold-finger cryostat exciting the samples with light pulses. These were obtained from either a mode-locked Nd-YAG laser, which synchronously pumped a cavity-matched dye laser, or a Ti:Zf mode-locked laser pumped by an $Ar^+$-ion laser. The pulse widths were 5 ps and 1.2 ps for the dye and the Ti:Zf systems, respectively. The incident light was directed along the growth axis of the heterostructures and a back-scattering geometry was used. The PL was time-resolved in a standard up-conversion spectrometer. The time resolution, obtained by overlapping on a non-linear crystal, $LiIO_3$, the luminescence from the sample with a delayed pulse from the laser, is basically determined by the temporal pulse width. A double-grating monochromator was used to disperse the up-converted signal. When necessary, the exciting light was circularly polarized by means of a $\lambda/4$ plate, and the PL was analysed into its $\sigma^+$ and $\sigma^-$ components using a second $\lambda/4$ plate placed before the non-linear crystal. Time delays at a given emission energy or time-resolved PL spectra at different delays after the excitation pulse have been obtained using this system.

For the spin relaxation of excitons we concentrate on the results for a GaAs/AlAs multi-quantum well, consisting of 50 periods of nominally 77 Å wide GaAs wells and 72 Å wide AlAs barriers. The sample was exceptionally bright and presented a small Stokes shift of $\sim$2.5 meV, which allowed us to perform quasi-resonant excitation at the free heavy-hole exciton, observed in pseudo-absorption experiments (PL excitation), detecting at the weakly bound exciton seen in PL. The influence of the exciton localization has been reported in the literature [55].

For the measurements of the electron spin relaxation, we have studied four p-type modulation-doped GaAs/GaAlAs quantum wells with hole sheet concentrations of $\sim 3 \times 10^{11}$ cm$^{-2}$, mobilities of $\sim$4000 cm$^2$ V$^{-1}$ s$^{-1}$ and well widths from 30 to 80 Å. The quantum well structures were grown either on [311] GaAs substrates and modulation doped with silicon or on [100] GaAs substrates and doped with beryllium. These structures were initially extensively tested with conventional, low-power, cw experiments [115]. In this work, we concentrate on the results obtained for a 30 Å thick QW modulation doped with beryllium. We have measured PL spectra at fixed times, as well as the PL decay at fixed emission energies, both as a function of temperature ($T = 10$–$50$ K) and as a function of the laser power, giving concentrations of excess carriers in the range between $\sim 10^{10}$ cm$^{-2}$ and $\sim 10^{11}$ cm$^{-2}$.

## 3. Results and discussion

### *3.1. Spin-flip processes of excitons and dark states*

In this work, the spin for excitons and/or holes is defined as the third component of the total angular momentum (for electrons in III–V semiconductors, this coincides with the usual concept of spin since their orbital angular momentum is zero; ‘s’ states). The spin relaxation of excitons between optically active states, with spin $\pm 1$, can take place in a single step, driven by the exchange interaction, or via a two-step process in which the individual constituents of the exciton, electron and hole, flip their spins separately, involving an intermediate dark state, with spin $\pm 2$. These paths are schematically depicted in figure 1. The rate of exciton spin relaxation in the latter, indirect channel is limited by the slower single-particle spin-flip rate, which usually is the electron one. Recent theoretical work on the spin relaxation of exciton-bound electrons shows that the coupling between optically active and inactive exciton states that differ only with respect to the electron spin direction represents an effective magnetic field that changes randomly as the exciton is elastically scattered and relaxes its spin [87]. In fact, this mechanism leads to a very similar process to that responsible for the DP mechanism [29].

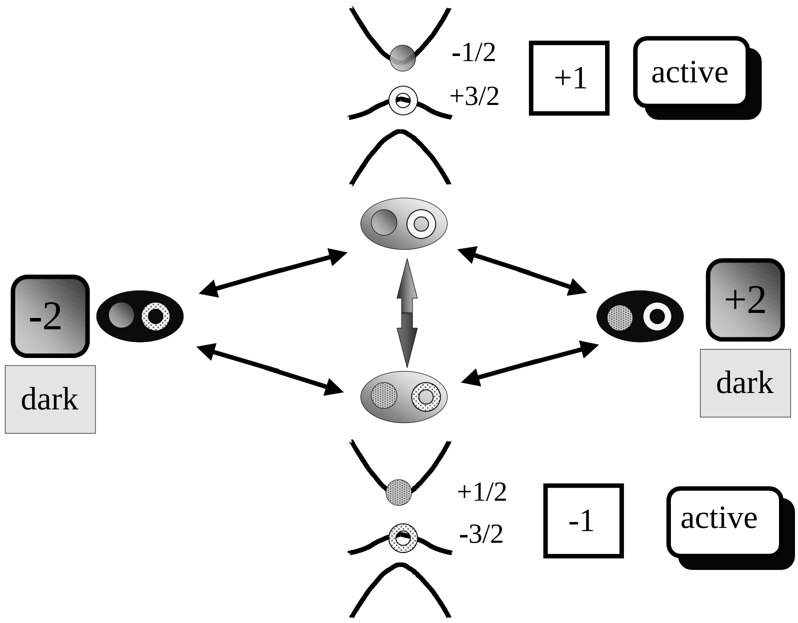


**Figure 1.** A schematic representation of the excitonic spin flip. An optically active $\pm 1$ exciton can flip its spin to $\mp 1$ in a single step (vertical path) or by sequentially flipping the spins of its fermions: first a hole and then an electron going from +1, passing through the dark state $-2$, to +1 (left-hand path), or first an electron and then a hole, passing through the dark state +2 (right-hand path).

In figure 2, we show the cw-PL (points) and the photoluminescence excitation (PLE) spectra (curve) of the sample studied. The spectra were recorded at 2 K under very low excitation density. The Stokes shift between the hh exciton peaks in PL and PLE amounts to 2.5 meV. On increasing the temperature, the Stokes shift decreases, and it vanishes at 40 K.

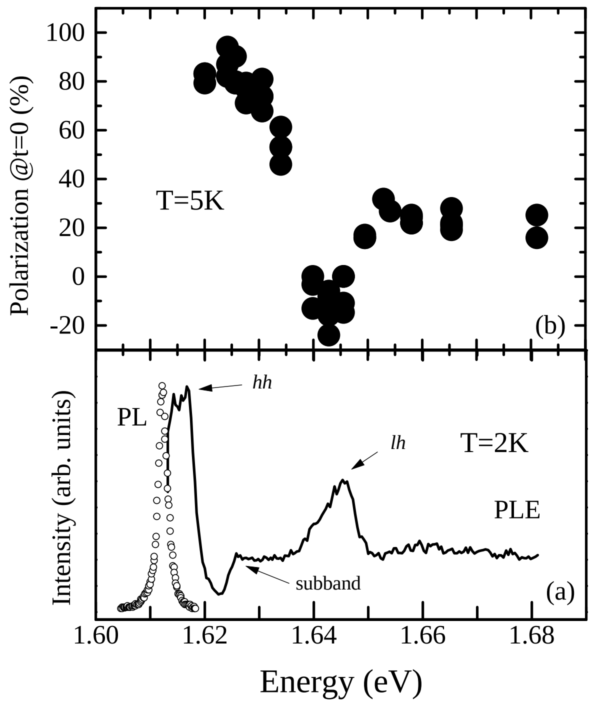


**Figure 2.** (a) Photoluminescence (open points) and excitation spectra (curve) of a 77 Å wide GaAs quantum well recorded at 2 K under an excitation of 5 mW $cm^{-2}$. The peaks are the heavy-hole (hh) and light-hole (lh) excitons. The step corresponds to the hh subband continuum. (b) The initial degree of polarization as a function of excitation energy obtained from TR-PL experiments at 5 K.

The linear temperature dependence of the decay time, which is characteristic of free excitons [116], also indicates that localization effects are not very important. The upper panel shows the initial value of the degree of polarization of the emission, which for a given helicity of the exciting light, i.e., $\sigma^+$, is defined as the fractional difference of the PL intensities of the two circular polarizations, $\sigma^+$ and $\sigma^-$,

$$P = (I^+ - I^-)/(I^+ + I^-).$$

These values were obtained at 5 K from TR-PL experiments exciting with $\sigma^+$-polarized light and analysing the two components of the emission. When exciting below the light-hole (lh) exciton, $P$ presents a marked dependence on energy, increasing as the excitation energy decreases. At the energy of the lh exciton, $P$ becomes negative and reaches a value of $\sim -20\%$. This negative value is due to excitonic effects, which enhance the creation of light holes and electrons with spin $+\frac{1}{2}$.

The time evolution of the PL for non-resonant excitation conditions is shown in figure 3. The dark points correspond to the emission of +1 excitons (with the same polarization as the exciting light), while the open points correspond to the annihilation of $-1$ excitons. Two main aspects are worth mentioning: in the first place, the depolarization of the excitons occurs during the rising of the intensity of the PL, while the initially created hot excitons are cooling down towards the lattice temperature; secondly, a very fast initial decay is observed in the black $\sigma^+$ trace. Several effects can give a fast initial decay of the exciton luminescence that are not related to the intrinsic radiative lifetime. Fast decays in the photoluminescence signal have been observed under resonant excitation conditions and have attributed to:

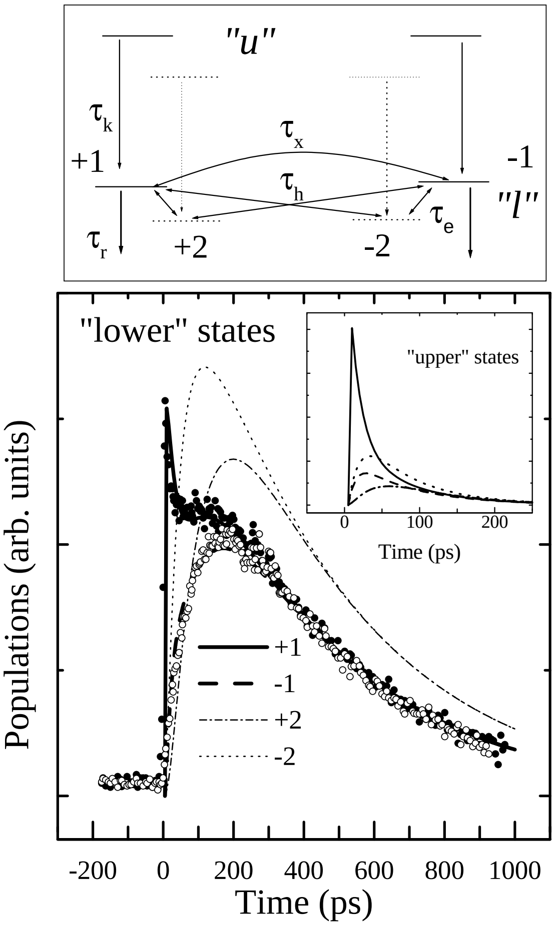


**Figure 3.** Time evolutions of the $\sigma^+$ (solid circles) and $\sigma^-$ (open circles) photoluminescence. The curves depict the best fits to a dynamical model based on the levels shown above the figure (see the text). The inset represents the populations for the upper states ('u') obtained from the fits.

(a) a very short radiative exciton lifetime; [117–119];
(b) scattering from $K = 0$ optically active excitons to $K > 0$, non-optically active, excitons [50, 118]; and
(c) relaxation of the spin of one of the fermions of the exciton, relaxing the total spin of the exciton from $\pm 1$ to $\pm 2$ [50, 56, 58, 59, 94, 118, 120].

Excitation under strictly non-resonant conditions rules out the first two explanations [56]. Therefore, only the transfer from optically active excitons to dark excitons can explain such as fast decay. It is worthwhile to mention that dark states have been observed directly in two-photon absorption measurements [121].

In the detailed study by Vinattieri *et al* it is demonstrated that in spite of the large number of parameters needed to model this decay, reliable values of relaxation rates can be extracted from a careful fitting procedure applied to the experimental curves [120]. The curves in figure 3 correspond to the best fit to a dynamical model based on the scheme shown in the upper part of the figure. It is assumed that an initial population of +1 excitons are created in the upper state (with $K > 0$); these have to relax ($\tau_k$) to the ground lower state ($K = 0$), before they recombine ($\tau_r$). During this time the excitons can flip the spin in a single step ($\tau_x$), or the electrons (holes) can flip their spins individually, $\tau_e$ ($\tau_h$). These spin-flip processes can happen in the ground and in the excited upper states. The energy separation between the dark, $\pm 2$, states and the active ones, $\Delta$, is given by the exchange interaction.

We find a value of $\Delta = 80$ $\mu$eV, in agreement with values reported in the literature [113, 122–124], but significantly smaller than the 200 $\mu$eV found in reference [58]. From our fitting, we also deduce that the active states lie above the dark states, in agreement with most of the other reports and in contradiction with the indications found in the time-resolved two-photon experiments [58]. Our value for $\tau_h = 25 \pm 8$ ps is compatible with others found in the literature [45], especially when the hole belongs to an exciton [47]. However, Vinattieri *et al* report larger values of $\tau_h = 100$–150 ps [120], and a much longer value of $\tau_h = 1$ ns has also been reported [66]. The value of $\tau_e = 320 \pm 100$ ps is similar to the value of 250 ps predicted theoretically for an 80 Å QW [87], and in agreement with the values found in experiments in the presence of an external electric field (from 333 ps to 3.3 ns) [120]. Finally, our fit obtains $\tau_k = 80 \pm 15$ ps and $\tau_x = 50 \pm 10$ ps. The latter value is in good agreement with the results of reference [120]; however, our value of $\tau_k$ is significantly higher than the value of 18 ps, previously reported in this reference, as can be expected from the fact that our excitation conditions are not in resonance with the hh exciton.

The thick (thin) curves in figure 3 correspond to the active (dark) excitonic populations (only the former can be observed in a one-photon emission experiment). The large population of $-2$ states manifests the importance of the rapid spin flipping of the holes which form the excitons. The inset in the figure depicts these populations for the $K > 0$, upper, excitons. Our results demonstrate that the transfer from optically active excitons ($\pm 1$) to dark ones ($\pm 2$) occurs also under excitation with circularly polarized light, in disagreement with the results of the Toulouse group [56, 59], who find this effect only when the exciting light is elliptically polarized.

All of these facts indicate that exciton dynamics is very complex, and is influenced by exciton recombination and momentum scattering and also by exciton, electron, and hole spin dynamics.

### *3.2. Spin splitting in a polarized exciton gas*

Figure 4 depicts TR-PL spectra taken at 8 K, 6 ps after excitation with $\sigma^+$ pulses for a density of $6.5 \times 10^{10}$ cm$^{-2}$, exciting at 1.625 eV. The grey area corresponds to the polarized ($\sigma^+$, spin +1) emission while the hatched one shows the unpolarized ($\sigma^-$, spin $-1$) PL. An energy splitting of $\sim$4.5 meV between the two peaks is clearly seen.

Increasing the excitation density, both a broadening of the lines and a strong enhancement of the splitting are obtained as shown in figure 5. The splitting is mostly due to the red-shift of the $\sigma^-$-polarized emission, and exhibits marked time and excitation energy dependences [93]. It has been contradictorily reported that the splitting is either due to the energy shift of the luminescence component with the same helicity of the laser pump, the other component being only slightly red-shifted [91], or due to the component of the opposite helicity [92]. Theory predicts that the absolute positions of the $\sigma^+$ and $\sigma^-$ emission components depend on the quasi-3D versus quasi-2D character of the semiconductor system [96]; recent unpublished experiments on double QWs demonstrate that those positions can be varied by an external electric field applied to the heterostructures [125]. One should also mention that, in this case, where the excitons become indirect in real space with drastically reduced electron–hole overlap, the spin-flip processes could be dominated by those of the electrons forming the excitons [87].

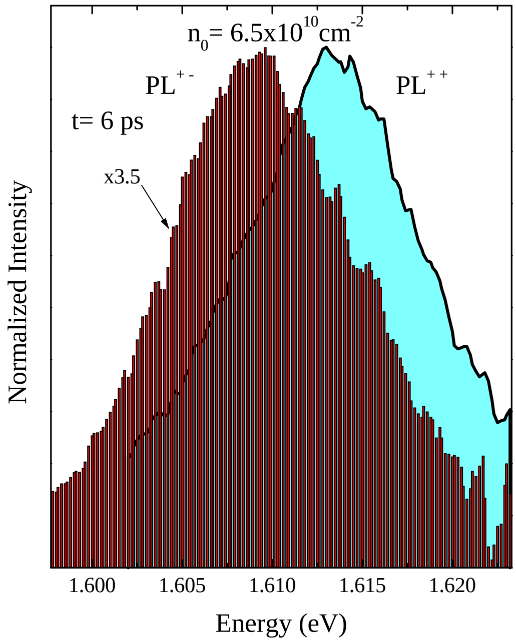


**Figure 4.** Low-temperature, 8 K, time-resolved PL spectra of the sample shown in figure 1 taken 6 ps after excitation with $\sigma^+$-polarized light at 1.625 eV. The grey (hatched) area depicts the $\sigma^+$ ($\sigma^-$) emission. The initial carrier density is $6.5 \times 10^{10}$ cm$^{-2}$. The $\sigma^-$ emission has been enlarged by a factor of 3.5.

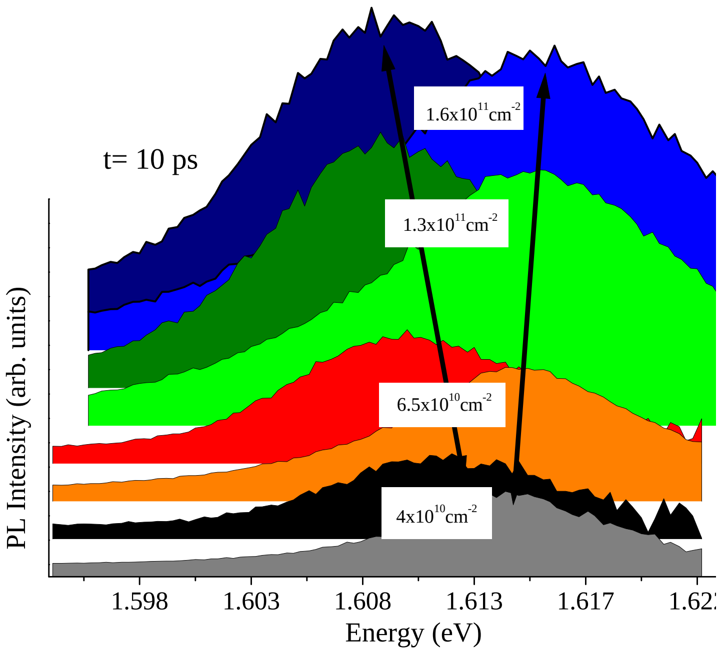


**Figure 5.** The evolution of the time-resolved PL spectra taken 10 ps after excitation for the 77 Å GaAs QW for different initial carrier densities. Each pair of spectra corresponds to a given initial carrier density; those spectra lying at higher (lower) energy depict the co-polarized, $\sigma^+$ (counter-polarized, $\sigma^-$) PL. The arrows indicate the blue-shift (red-shift) of the $\sigma^+$ ($\sigma^-$) PL.

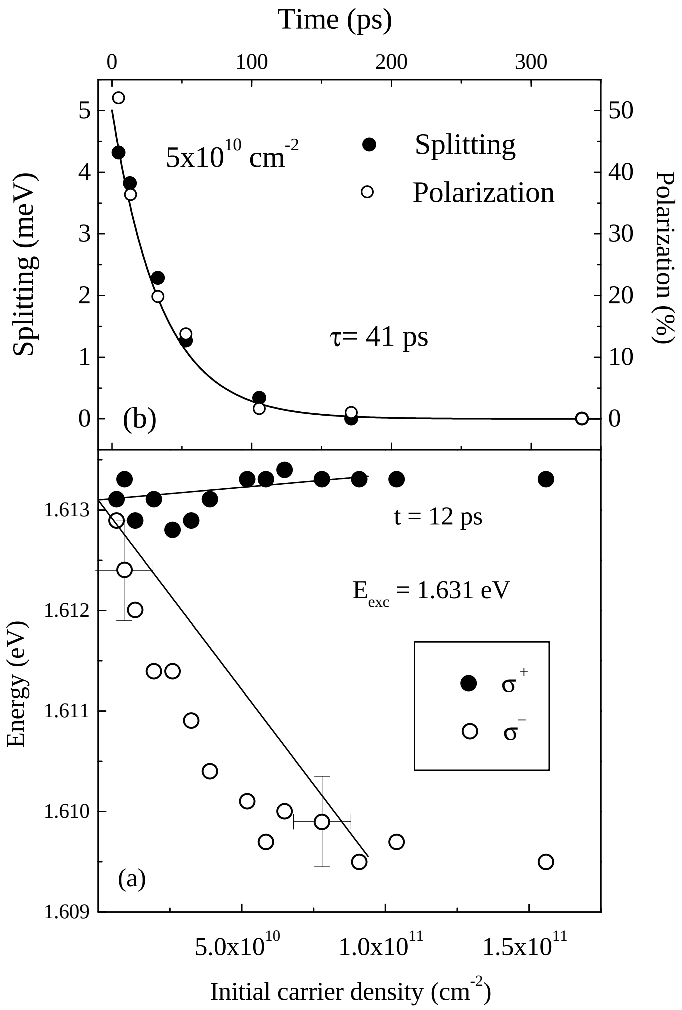


**Figure 6.** (a) Energies of the co-polarized ($\sigma^+$, solid points) and counter-polarized ($\sigma^-$, open points) luminescence as functions of the initial carrier density. The positions are taken 12 ps after excitation at 1.631 eV. The curves represent the results obtained using equation (1). (b) The time evolution of the PL splitting (solid points) and polarization (open points) for an initial carrier density of $5 \times 10^{10}$ cm$^{-2}$. The line shows the best fit to an exponential decay with a time constant of 41 ps.

Figure 6(a) depicts the dependence of the energy positions of the PL on the initial carrier density (open and solid points). Under the conditions presented in this figure, 12 ps after excitation at 1.631 eV, the $\sigma^+$ emission remains practically constant, while the $\sigma^-$ emission red-shifts with increasing carrier density up to $9 \times 10^{10}$ cm$^{-2}$. The curves correspond to a model which takes into account inter-excitonic exchange interaction and screening [96]. This model gives the *changes* in the energies of the interacting $\pm 1$ excitons as a function of the total and the $\pm 1$ populations of excitons as follows:

$$E^{\pm}\ (\mathrm{eV}) = 2.214 \times 10^{-16} a\ (\text{Å}) \left[1.515 n^{\pm}\ (\mathrm{cm}^{-2}) - 0.41 \pi n\ (\mathrm{cm}^{-2})\right]. \qquad (1)$$

For the curves in figure 6(a), the energy of a single exciton has been taken from the experimental energy of the +1 exciton at the lowest carrier density; a three-dimensional Bohr radius, $a$, of 150 Å and an initial degree of polarization of 80% have been used. In spite of the strong approximations used in the theory, such as neglecting the presence of dark, $\pm 2$, states and assuming that the excitons are all at $K = 0$, which are not borne out by our measurements, the agreement with the experiments is satisfactory.

The splitting is strongly correlated with the degree of polarization of the exciton gas, as can be observed in figure 6(b), which depicts the time evolution of the splitting and $P$. This has also been confirmed by experiments where the degree of polarization of the exciting light has been varied from circular to linear [92]. This correlation is also predicted by the theory: equation (1) shows that the splitting is proportional to the difference between exciton +1 ($n^+$) and $-1$ ($n^-$) populations and thus proportional to the degree of polarization ($P = (n^+ - n^-)/(n^+ + n^-)$). When $n^+$ and $n^-$ become similar, and therefore $P$ approaches zero, the splitting disappears as a consequence of the convergence of the $\pm 1$ excitons towards the same energy, as predicted by equation (1). The time decay of $P$ originates from the excitonic spin-flip processes described in section 3.1, which are mainly driven by intra-excitonic exchange interaction (the Bir–Aronov–Pikus, BAP, mechanism) [45].

Additionally, it has also been observed, under resonant excitation, that the luminescence component co-polarized with the laser excitation is narrower than the counter-polarized one, despite the much higher density of +1 excitons [70]. The linewidth difference decreases with time due to the decay of the PL polarization.

### *3.3. Spin polarization of an optically pumped electron gas*

The time evolution of the two spin components of a photocreated 2DEG is investigated as a function of the density of carriers excited with a picosecond laser pulse [69]. Exciting a p-type GaAs quantum well below the lh resonance, electrons with almost purely one spin component are photocreated. The filling of the conduction band is clearly different for the two electron spin components, leading to an appreciable shift between $\sigma^+$ and $\sigma^-$ emission spectra. The decay of the spin polarization of the electron gas is found to depend strongly on the excitation power: an usual monoexponential decay of the spin polarization (with a characteristic time of 550 ps) is observed at low powers, whereas a fast depolarization process (with a characteristic time of 20 ps) turns on progressively when the density of photocreated carriers approaches the concentration of holes originating from doping. The observation of the fast component (typical for the relaxation of the hole magnetic moment) in the electron spin relaxation suggests that this is driven by the decay of the total polarization of the hole gas. Such a process may only be expected at sufficiently high excitation powers, when the concentration of photocreated, spin-polarized holes becomes comparable with the density of non-polarized holes arising from doping.

Figure 7 depicts the PLE spectra of a 30 Å [100]-oriented QW at 2 K, excited with $\sigma^+$-polarized light recorded at the tail of the PL. The onset of the absorption due to the hh transition is clearly seen as a peak in the $\sigma^+\sigma^+$ spectrum at 1.7 eV, while the one corresponding to the lh transition is dominant in the $\sigma^+\sigma^-$ spectrum at 1.738 eV. As can be deduced from this figure, the sample shows a high degree of optical alignment, indicating a long spin-flip-relaxation time for the photoexcited electrons. This is even more clearly seen in the inset of the figure, which displays the cw-PL of a [100] QW, 50 Å wide, at different lattice temperatures. The thick (thin) curves correspond to the emission co-polarized (counter-polarized) with the exciting light. A very large degree of polarization is observed at the lowest $T$ and it diminishes as the temperature is increased. For excitation energy above the threshold of lh states, the polarization decreases rapidly, since electrons with opposite spin directions are produced from the light-hole subband.

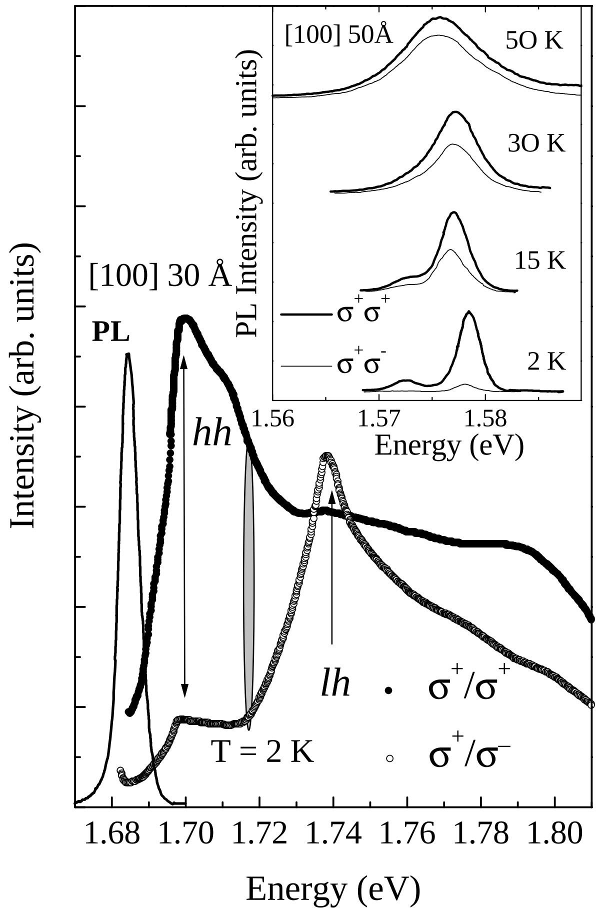


**Figure 7.** PL (solid curve) and excitation spectra of a 30 Å thick p-type modulation-doped ($p = 3 \times 10^{11}$ cm$^{-2}$) QW measured for aligned (solid points) and crossed (open symbols) polarization of the exciting/emitted light. The shaded area indicates the energy used for excitation in the time-resolved experiments. The inset displays cw-PL spectra of a similar heterostructure, a QW 50 Å thick, for different lattice temperatures and polarization configurations: aligned: thick curves; crossed: thin curves.

Large values of $P$ have already been reported for p-doped strained films [126], quantum wells [127], and superlattices [128]. An extremely long electron spin-relaxation time of 20 ns, two orders of magnitude longer than that found for homogeneously doped GaAs for comparable acceptor concentrations, has been found for p-type $\delta$-doped GaAs:Be/AlGaAs double heterostructures and has been attributed to a drastic reduction of the electron–hole wavefunction overlap, which strongly reduces the electron–hole exchange interaction [67]. In II–VI-based QWs, $Zn_{1-x}Cd_xSe$/ZnSe, the introduction of electrons by modulation doping increases the electronic spin lifetimes by several orders of magnitude relative to the insulating counterparts, a trend that is also observed in bulk semiconductors [104, 105]. The spin lifetime exceeds the recombination time by nearly two orders of magnitude, suggesting that the 2DEG acquires a net polarization either through energy relaxation of spin-polarized electrons or through angular momentum transfer within the electronic system. These studies also show that the nanosecond spin-flip times persist up to room temperature. Also for excitons, spin-flip times exceeding the radiative recombination lifetime have been observed in InGaAs quantum discs [62].

Using these p-type samples, we can easily investigate spin-alignment effects in the conduction band: electrons with an unbalanced population of the two spin components, created under circularly polarized excitation, recombine with non-polarized holes which mostly originate from doping. Therefore the spin relaxation of the electrons can be obtained from the difference of the time evolution of the two orthogonally polarized emissions. The spin-relaxation time of photogenerated electrons in p-doped QWs has been calculated by Maialle and Degani [79]. They have found that, for the mechanism of exchange interaction, the spin mixing of the valence hole does not play an important due to a compensation between the enlargement of the hole density of states and a spin-mixing-induced decrease of the exchange strength.

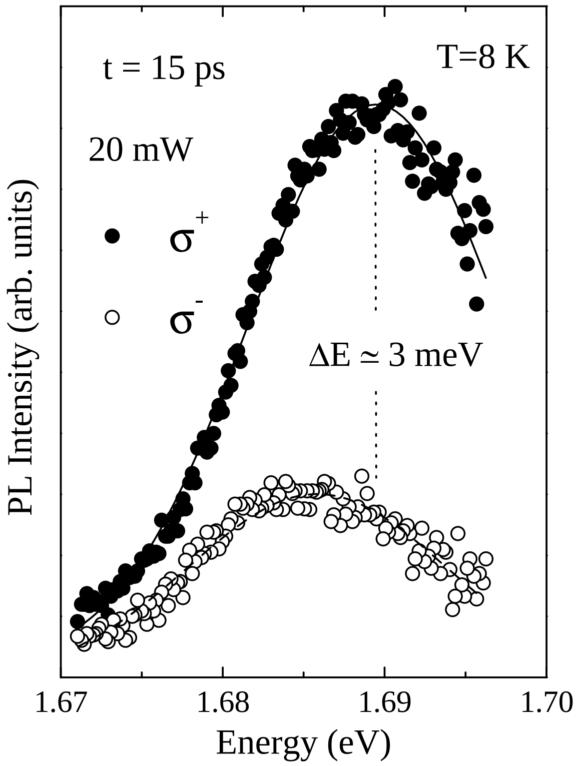


**Figure 8.** Co-polarized (solid points) and counter-polarized (open points) components of the PL spectra of the sample shown in figure 7, measured at 15 ps after a $\sigma^+$-polarized pulsed excitation with a mean laser power of 20 mW and excitation energy of 1.717 eV. Bath temperature: 8 K.

In an ideal system, using the estimated hole Fermi energy of 2 meV for our sample, and assuming a ratio of six between the hole and electron effective masses, the circularly polarized luminescence spectra are expected to directly reflect the distributions of electrons with different spin components in an energy range up to $\sim$12 meV above the conduction band edge. However, as shown in figure 8, the spectra measured at 15 ps after a 20 mW excitation cover a somewhat wider spectral range. We assume that even these spectra probe only the properties of the electron gas, since the sample investigated shows an appreciable spectral broadening already under low-power cw excitation (half-width of the luminescence: $\sim$10 meV; see figure 7).

Figure 8 represents the $\sigma^+$ and $\sigma^-$ components of the luminescence spectra excited with $\sigma^+$ pulses at 1.717 eV. These spectra clearly show the difference between the occupations of electronic states with opposite spins. This difference, which vanishes at longer delay times, leads to the energy difference between the positions of the maxima in the $\sigma^+$ and $\sigma^-$ luminescence spectra.

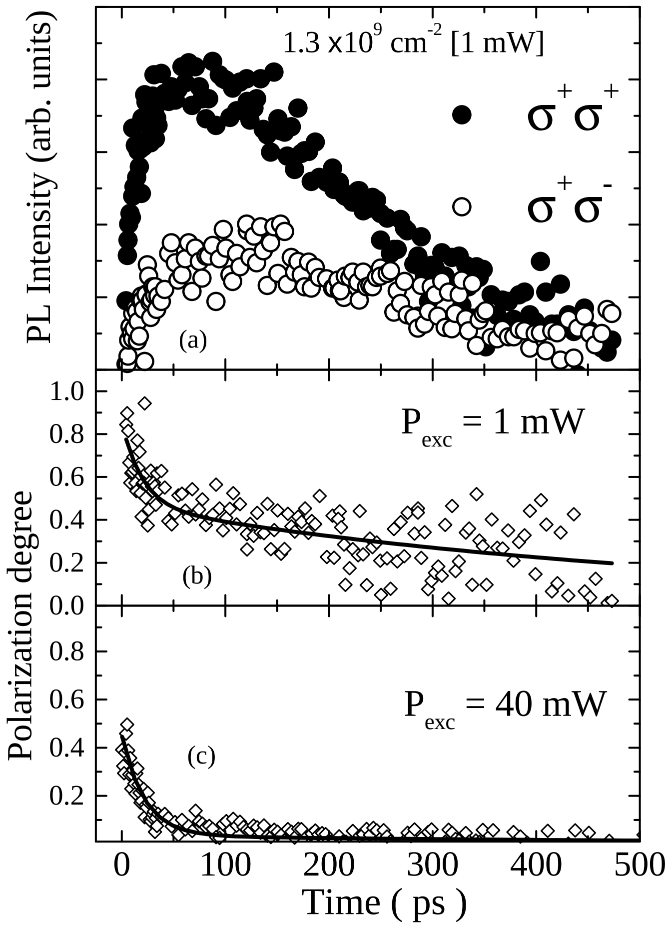


**Figure 9.** (a) The decay of $\sigma^+$ (solid points) and $\sigma^-$ (open points) luminescence under pulsed $\sigma^+$ excitation with a mean laser power of 1 mW. (b) Time evolution of the degree of polarization for 1 mW mean laser power. (c) As (b), but for a laser power of 40 mW. The curves represent the best fits according to the sum of two exponential decays: $Ax\ \exp(-t/\tau_1) + Bx\ \exp(-t/\tau_2)$. The sample is the same as for figure 7.

The most conspicuous finding is illustrated in figure 9: panel (a) shows the evolution of the two components of the polarized PL and panels (b) and (c) depict the time evolution of the degree of polarization, $P$, for two different powers of the exciting light. We have found that the decay of the spin polarization of the electron gas depends very much on the intensity of the laser excitation. The decay of the degree of luminescence polarization, $P$, measured at $T = 8$ K can be well reproduced by a sum of two exponential decays with two distinct characteristic times of $\tau_1 = 20$ ps and $\tau_2 = 550$ ps. The amplitude of the fast component vanishes at low excitation power, whereas this fast process almost completely determines the electron spin depolarization at the highest level of laser excitation. It is well known that for any mechanism of electron spin relaxation [29], the probability of spin-flip transitions increases as a function of the electron $k$-vector. Therefore, the increase in the rate of spin relaxation as a function of the laser power may result partially from a larger electron kinetic energy caused either by an increase of the effective electron temperature or of the initial electron concentration. However, this simple reasoning hardly explains our data. From an analysis of the time evolution of the luminescence spectra, we have estimated an increase in the mean kinetic energy of the electron gas of only 4 meV at the highest laser power. This amount is not sufficient to reduce the spin-relaxation time down to 20 ps, since at low excitation powers but high lattice temperatures ($kT \sim 3.44$ meV) we still observe a relatively long spin-relaxation time ($\sim$80 ps).

We have simulated measured spectra at different times after the excitation, $I^{+(-)}(\hbar\omega)$, by the broadened convolution of Fermi–Dirac statistics for a non-polarized gas of holes and two spin components of the 2DEG, assuming the conservation of $k$-selection rules:

$$I^{+(-)}(\hbar\omega - E_g) = I^{+(-)}(E_e + E_h) = A \int_0^\infty f_{E_e}^{+(-)} f_{E_h} G_\Gamma(E_e - E_e)\delta(\vec{k}_e - \vec{k}_h)\, \mathrm{d}E_e. \qquad (2)$$

Here $E_g$ is the energy gap; e (h) stands for electrons (holes); $I^{+(-)}$ denotes the intensity of $\sigma^+$ ($\sigma^-$) luminescence, $G_\Gamma(x)$ is a Gaussian broadening function with a broadening parameter, $\Gamma$, of 7 meV, chosen to reproduce the low-temperature (4 K), low-power (1 mW cm$^{-2}$) cw spectra, and

$$E_{e(h)} = \hbar k_{e(h)}^2/2m_{e(h)}$$

is the electron (hole) energy, where we assumed $m_e = 0.075m_0$ and $m_e/m_h = 0.18$.

An analysis of pairs of $\sigma^+$ and $\sigma^-$ PL spectra leads us first to conclude that each component is well described by assuming a common temperature for the two electron spin components (and for holes), but different values of the chemical potential. Excluding very short delay times after excitation, i.e., already after a few picoseconds, each spin component of the 2DEG can be qualitatively characterized by its own Fermi distribution, each one with a different chemical potential but both with very similar temperatures. It could be argued that due to differences in the exchange interaction, the unbalanced populations of the two spin components could also induce a difference in the many-body renormalization between occupied electronic states with opposite spins. We have systematically observed that the low-frequency onset of the emission associated with the majority spins always occurs below the corresponding onset of the minority-spin luminescence. This effect is, however, rather weak, as can be seen from the spectra shown in figure 8. This means that, under our experimental conditions, the exchange interaction of the electrons is unable to stabilize a common chemical potential of the electron gas for the two spin components. This latter situation might be expected under equilibrium conditions, and would imply a difference between the renormalizations of the conduction band edges for the two spin components. On the other hand, the attainment of a common temperature for electrons and holes in a very short time is expected, and this is well documented in the literature [129].

To fit our measurements with equation (2), we assumed that the time evolution of the total electron concentration follows the decay of the total luminescence intensity observed at sufficiently long delay times, i.e., $n = n^+ + n^- = N_0 \mathrm{e}^{-t/230 \text{ ps}}$, in the case of the 10 mW series. The initial electron concentration, $N_0 = 15 \times 10^{10}$ cm$^{-2}$, was found by a self-consistent fitting of several spectra measured at long delay times, and agrees within a factor of 2 with an estimation based on the absorption coefficient and the laser power density on the samples. The hole concentration was assumed to be $n_h = n^+ + n^- + n_h^0$, where $n_h^0 = 3 \times 10^{11}$ cm$^{-2}$ originates from modulation doping. The electron concentrations $n^{+(-)}$, which define the corresponding chemical potentials, were determined from the experiment assuming $n^+/n^-$ to be equal to the ratio of the integrated intensities of the $\sigma^+$ and $\sigma^-$ PL. Finally, a given pair of $\sigma^+$ and $\sigma^-$ spectra were fitted with just two parameters: the carrier temperature and a proportionality factor, $A$, which was found to be common to all of the simulated spectra, within experimental error.

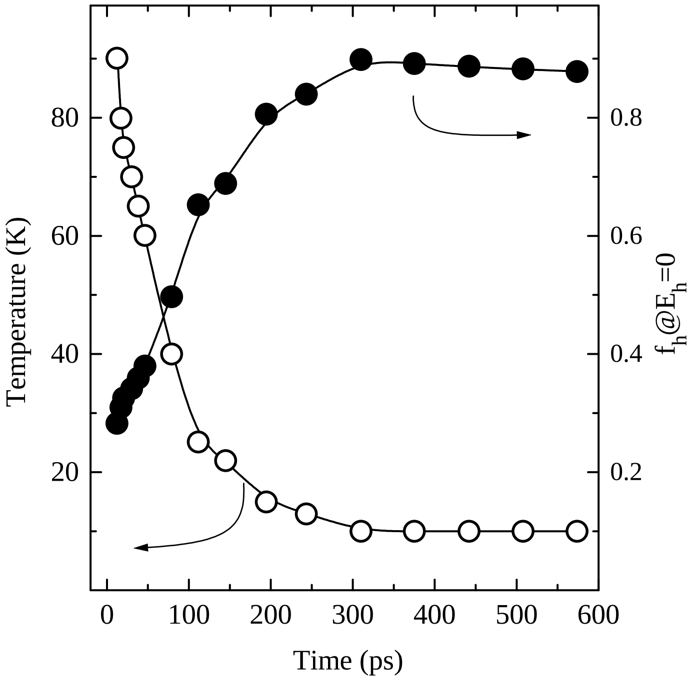


**Figure 10.** The time evolution of the carrier temperature (open circles), for a mean laser power of 10 mW, obtained from the fits of the time-resolved spectra using equation (2) (see the text). The sample is the same as for figure 7. The solid symbols depict the time evolution of the number of occupied hole states at the top of the valence band ($f_h$ at $E_h = 0$).

The time evolution obtained for the carrier temperature is shown in figure 10 (open circles). The carrier temperature rises up to $\sim$100 K just after the laser pulse. This fact, in conjunction with the measurements as a function of lattice temperature (see section 3.4), accounts for the fast depolarization of the electronic spins, induced by the laser power. Our results confirm the high efficiency of carrier–carrier interaction in establishing a common temperature for electrons and holes. Cold before excitation, the gas of holes becomes non-degenerate almost immediately after the laser pulse. This non-degenerate character of the hole gas is illustrated in figure 10 (solid circles), where the number of occupied hole states at the top of the valence band is plotted as a function of time.

High carrier temperatures, and the associated fast depolarization of the electronic spins, shortly after high-power pulsed excitation, are not very surprising, though we show that the degree of spin polarization is a sensitive measure of carrier temperature. On the other hand, it is interesting to note that at long delay times (low carrier temperature), we always observe a slow spin relaxation, independently of the excitation power, i.e., electron concentration. From the spectral simulation we have, for example, concluded that, for an excitation with 40 mW power and 175 ps after the laser pulse, the carrier temperature is 15 K and the electron concentration is $2.5 \times 10^{11}$ cm$^{-2}$. Under these conditions both electrons and holes are degenerate and electrons flip their spins in the vicinity of their chemical potentials (which are slightly different for the spin-up and spin-down components). The electrons flipping spins have high kinetic energies ($E_F/k = 90$ K); however, the observed spin-relaxation time remains long. This is in contrast to the case of fast spin relaxation (short times) when the electrons flipping spins also have high kinetic energies (raised by an increase of their temperature), but the carrier distributions are more Boltzmann-like.

Bir *et al* have established that the rate of electron spin relaxation due to holes is proportional to the time of interaction with the holes, i.e., the time during which the distance between them is less than the electron wavelength [32]. Under conditions for which this time equals the time of diffusion of holes through the interaction region, strong scattering of holes leads to a decrease in the electron spin-relaxation time. On the other hand, under conditions for which the hole spin-relaxation time becomes less than the interaction time, strong hole spin relaxation leads to a decrease in the electron spin-relaxation rate due to an efficient averaging of the hole spin. Therefore, the non-degenerate character of the electrons and holes, and their high temperatures, shortly after excitation can lead to the very rapid electron spin relaxation found in our experiments.

We therefore conclude that fast spin depolarization in our structures is driven by the non-degenerate character of carrier distribution and not exclusively by the increase of the electron kinetic energy. Such behaviour can be understood in terms of the BAP mechanism of the electron spin relaxation but it is hardly accounted for by the DP processes whose efficiency is directly related to the electron kinetic energy. As can be deduced from our previous discussion, non-degenerate carrier distributions favour the efficiency of spin-flip electron scattering via the exchange interaction with holes; in contrast, the available number of scattering configurations is appreciably reduced for the degenerate systems. Similar results could also be expected for n-doped samples, which have been shown recently to have long electronic spin lifetimes [104], although the very fast spin relaxation of photocreated holes [45] would render the experiments much more difficult.

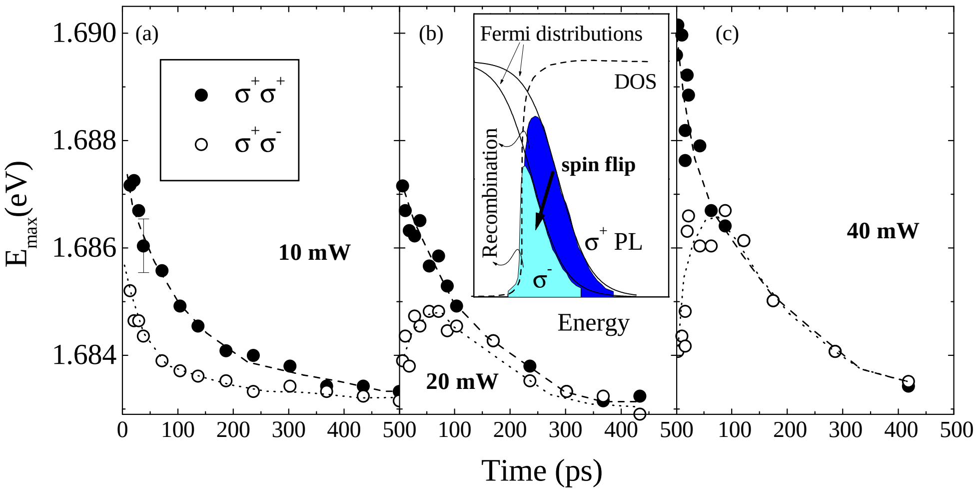


**Figure 11.** Energy positions of the PL maxima for co-polarized (solid points) and counter-polarized (open symbols) emission as a function of the time delay after a pulsed $\sigma^+$ excitation for a mean laser power of: (a) 10 mW; (b) 20 mW; and (c) 40 mW. The sample is the same as for figure 7. The inset shows schematically the Fermi distributions, the 2D density of states (DOS), and the corresponding electron $+\frac{1}{2}$ (dark area) and $-\frac{1}{2}$ (light area) populations, which decay either by recombination (thin, solid arrows) or spin flipping (thick arrow).

The splitting in the PL maxima is linked to the differences between the Fermi energies of spin-up and spin-down electrons. Its time evolution and power dependence is strongly connected to the spin-flip dynamics. Figure 11 depicts the energy of the maxima of the PL for different excitation powers as a function of time delay after the pulsed excitation. At 10 mW, both the co-polarized (solid points) and the counter-polarized (open points) emissions red-shift with time and the splitting vanishes at ∼400 ps. On doubling the power, a distinct behaviour is found for the $\sigma^-$ emission, which blue-shifts during the first ∼75 ps; the splitting disappears now at ∼250 ps. This time is further reduced to ∼75 ps when the power is again augmented by a factor of two, and the blue-shift of the $\sigma^-$ PL lasts until the energy positions of the two polarizations merge. Additionally, it is observable in the figure that the initial splitting, at $t \sim 0$, increases from ∼2 meV (10 mW) to ∼6 meV (40 mW). The inset in the figure gives a qualitative description of the splitting. Initially a larger population of $+\frac{1}{2}$ electrons is created by the $\sigma^+$ pulse compared to that of $-\frac{1}{2}$ electrons, and therefore $E_F(+\frac{1}{2}) > E_F(-\frac{1}{2})$. The recombination processes (curved solid arrows) lower the populations of both kinds of electron, and thus also decrease their Fermi energies, and a red-shift of both emissions results. However, the spin-flip processes (thick arrow) decrease (increase) the populations of $+\frac{1}{2}$ $(-\frac{1}{2})$ electrons. Depending on which process, recombination versus spin flipping, is faster, a red- or blue-shift of the $\sigma^-$ emission is obtained, while the $\sigma^+$ PL will always red-shift. On increasing the power, the fast channel for spin flipping (20 ps) becomes more important, and since it is much faster than the recombination (230 ps) a blue-shift is obtained for $\sigma^-$ PL. In contrast, at low powers the spin flipping becomes slower (550 ps) than the recombination, and both co-polarized and counter-polarized emissions red-shift.

This finding of two different quasi-Fermi levels could have important consequences for possible ultrafast devices based on spin-polarized transport in hybrid magnetic semiconductor systems. Experiments on transport through non-magnetic metal sandwiched between two ferromagnetic films have shown that is valid to assume that the current is carried by two non-intermixing components, with spin up and spin down, and that one need only determine the spin-scattering coefficient for each of these components to completely describe the magnetoresistance behaviour of a multilayered structure [1]. A spin transistor (emitter and collector: ferromagnetic films; base: non-magnetic metal), which is based on the shift of the chemical potential due to the accumulation of spin-polarized electrons in a normal metal, has also been demonstrated [130].

### *3.4. Temperature dependence of the electron spin flipping*

Figure 12 shows the PL dynamics for different lattice temperatures at a photocreated electron density of $2.6 \times 10^9$ cm$^{-2}$. On increasing $T$, a large increase of the decay time, $\tau_d$, is observed from 195 ps at 5 K to 475 ps at 60 K. This increase is attributed to heating of the carriers due to electron–phonon scattering, which moves the electrons out of the emission region, therefore competing with the radiative recombination processes. Furthermore, with increasing lattice temperature $T$, the electron and hole distribution functions broaden, yielding a smaller density of occupation and thus decreasing the PL intensity as can be readily seen in figure 12. The rate of increase of $\tau_d$ is independent of the growth direction, but increases considerably with increasing QW width, for an 80 Å QW attaining $\tau_d = 780$ ps at 60 K.

The time evolution of the degree of polarization, $P$, at 8 K for the [100] QW, exciting at 1.717 eV and detecting at the PL peak, is shown in figure 13(a) for a photocreated electron density of $5.3 \times 10^9$ cm$^{-2}$. It is clearly seen that the decay is not monoexponential, indicating the presence of different spin-flip mechanisms. A fit with the sum of two exponential decays (the curves in figure 13(a)) yields spin-flip times of $\tau_1 = 20$ ps and $\tau_2 = 550$ ps. The fast time,

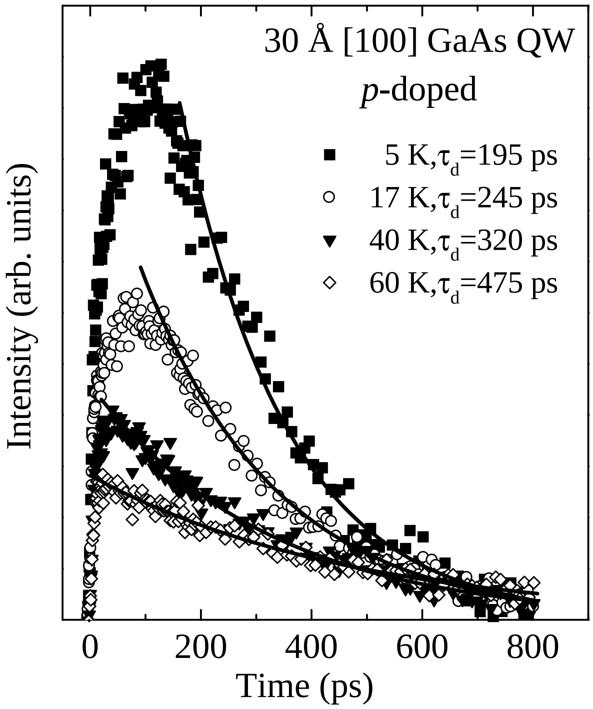


**Figure 12.** PL time evolutions for different lattice temperatures of the 30 Å wide, modulation-doped QW shown in figure 7. The curves are best fits to exponential decays, with various decay times $\tau_d$.

$\tau_1$, is attributed to the non-degenarate character of the holes almost immediately after the laser pulse. This carrier distributions was shown in the previous section to favour the efficiency of spin-flip electron scattering via the exchange interaction with holes. The slow time, $\tau_2$, corresponds to the spin flipping of electrons in the presence of a degenerate hole gas; it is important to note that $\tau_2$ is a factor of two longer than the PL decay time, $\tau_d$. Both spin-flip times are independent of the excitation power, but the contribution to the spin relaxation of the fast mechanism increases with the power. On increasing $T$, both spin-flip mechanisms speed up considerably. A fit at 40 K yields values of 10 ps and 80 ps for $\tau_1$ and $\tau_2$, respectively. We will concentrate in the following on $\tau_2$, which we identify as the intrinsic spin-flip time of electrons, $\tau_{sf}$.

For bulk GaAs the temperature dependence of the spin flipping of electrons has been studied in great detail by Fishman and Lampel [15], who found that at low temperature the exchange interaction with the holes is the dominant relaxation mechanism. On the other hand, at higher temperatures ($T \geqslant 100$ K), and low acceptor concentrations, the DP mechanism governs the electron spin relaxation. This mechanism is important only at high temperatures in 3D systems, because only then does the thermal activation of the carriers impel them to 'feel' the non-parabolicity of the conduction band [17]. However, in 2D systems, this mechanism should be more effective for thinner wells, where the quantum confinement effects are more marked, and therefore should be noticed at lower temperatures than in bulk. This has been observed in TR-PL measurements on p-doped GaAs QWs of different thicknesses [68]: for 180 Å wide wells no clear dependence of the spin-flip time on temperature was found; however, for 55 Å wells the DP mechanism was found to dominate for temperatures as low as 7 K. It

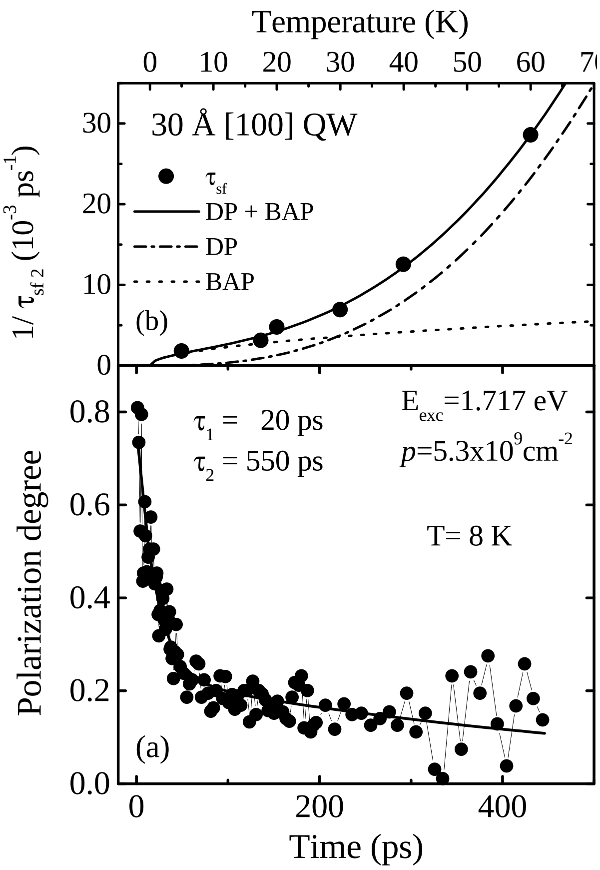


**Figure 13.** (a) The time evolution of the degree of PL polarization of the sample shown in figure 7. The curves represent the best fits according to the sum of two exponential decays, similarly to those in figure 9. (b) The temperature dependence of the spin-flip rate of the slow channel, $\tau_2$; the curves are the fits to different spin-flip mechanisms (see the text).

should also be mentioned that in spite of the large excitation powers used in that work [68], only a single, very long spin-flip time of the order of 1 ns at low temperatures is reported, in contrast with the two channels that we find for our samples.

The $T$-dependence of the spin-flip rate, $1/\tau_{sf}$, is depicted using solid points in figure 13(b). It allows the identification of the spin-flip mechanisms: for the BAP mechanism, a $T^{1/2}$-dependence is expected [32], while for the DP mechanism a $T^{\alpha}$-dependence is predicted [29, 75]. The best fit of our data to those laws (curves in figure 13(b)) gives $\alpha = 2.6 \pm 0.3$, and proves that, similarly to the case for electrons in bulk, the spin-flip processes of two-dimensional electrons are governed by the exchange mechanism at low temperatures, while the DP mechanism takes over at higher temperatures. Furthermore, from our data a momentum scattering rate with a $\sim T^{-1/2}$-dependence is deduced. This value of $\alpha$ is also compatible with the fact that the spin flipping of electrons takes place in a region of strong hole spin relaxation [32]. Finally, let us mention that the temperature dependence of the excitonic spin flipping in intrinsic QWs is still not well understood: although exchange interaction (the BAP mechanism) is believed to be the main spin-flip mechanism, it is found that $\tau_{sf}$ is independent of $T$ at low temperatures (4 K $< T <$ 30 K) [55, 58].

## 4. Summary

We have shown that spin-flip processes in 2D systems constitute a very active field of research and that many questions are still open to further investigation. In particular, we have shown that for excitons the main spin-flip mechanism is intra-excitonic exchange (the BAP mechanism), although spin flipping of the individual fermions forming the exciton is responsible for fast decays observed in the TR-PL emission. Inter-excitonic exchange is shown to generate a splitting of the excitons in a polarized gas. In the case of a 2DEG, the spin flipping of electrons is driven by the BAP and DP mechanisms at low and high temperatures, respectively. When this gas is created with a net spin polarization by means of optical orientation, and becomes dense, then strong effects, non-linear in the excitation power, are observed in the polarization of the emission, which originate from the non-degenerate character of the carrier distribution shortly after the laser excitation. An optically aligned, spin-polarized electron gas can be well described by two separate Fermi–Dirac distribution functions, one for each spin component, with a common temperature but different chemical potentials.

## Acknowledgments

This work would not have been possible without agreeable collaboration with many people, especially with: L Muñoz, E Pérez, J Fernández-Rossier and C Tejedor, who did great work in the study of excitons. The studies of 2DEGs were motivated by a collaboration with M Potemski and L Gravier; M D Martín contributed considerably to these studies. All of the samples mentioned in this article were kindly provided by K Ploog. This research was partially supported by the Fundación Ramón Areces, the Spanish DGICYT (contract PB96-0085), and the CAM (contract 07N/0026/1998)

## References

[1] Prinz G A 1995 *Phys. Today* **48** 58
[2] Monsma D J, Vlutters R and Lodder J C 1998 *Science* **281** 407
[3] Nishikawa Y, Takeuchi A, Yamaguchi M, Muto S and Wada O 1996 *IEEE J. Quantum Electron.* **2** 661
[4] Ando H, Sogawa T and Gotoh H 1998 *Appl. Phys. Lett.* **73** 566
[5] Hanle W 1924 *Z. Phys.* **30** 93
[6] Fleisher G, Dzhioev R I, Zakharchenya B P and Kanskaya L M 1971 *JETP Lett.* **13** 299
[7] D'yakonov M I and Perel' V I 1976 *Sov. Phys.–Semicond.* **10** 208
[8] Vekua V B, Dzhioev R I, Zakharchenya B P and Fleisher V G 1976 *Sov. Phys.–Semicond.* **10** 210
[9] Pikus G E and Ivchenko E L 1982 *Excitons* vol 6, ed E I Rashba and M D Sturge (Amsterdam: North-Holland) p 205
[10] Seymour R and Alfano R R 1980 *Appl. Phys. Lett.* **37** 223
[11] Seymour R J, Junnakar M R and Alfano R R 1981 *Phys. Rev.* B **24** 3623
[12] Johnson E J, Seymour R J and Alfano R R 1984 *Semiconductors Probed by Ultrafast Laser Spectroscopy* vol 2, ed R R Alfano (New York: Academic) p 200
[13] Clark A H, Burnham R D, Chadi D J and White R M 1975 *Phys. Rev.* B **12** 5758
[14] Clark A H, Burnham R D, Chadi D J and White R M 1976 *Solid State Commun.* **20** 385
[15] Fishman G and Lampel G 1977 *Phys. Rev.* B **16** 820
[16] Zakharchenya B P, Mirlin D N, Perel' V I and Reshina I I 1982 *Sov. Phys.–Usp.* **25** 143
[17] Zerrouati K, Fabre F, Bacquet G, Bandet J, Frandom J, Lampel G and Paget D 1988 *Phys. Rev.* B **37** 1334
[18] Kikkawa J M and Awschalom D D 1998 *Phys. Rev. Lett.* **80** 4313
[19] Gross E F, Ekimov A I, Razbirin B S and Safarov V I 1971 *JETP Lett.* **14** 108
[20] Weisbuch C and Fishman G 1976 *J. Lumin.* **12+13** 219
[21] Planel R and Benoît a la Guillaume C 1984 *Optical Orientation* vol 8, ed F Meier and B P Zakharchenya (Amsterdam: Elsevier) p 353
[22] Zemskii V I, Zakharchenya B P and Mirlin D D 1976 *JETP Lett.* **24** 82

[23] Zakharchenya B P, Zemskii V I and Mirlin D N 1977 *Sov. Phys.–Solid State* **19** 1006
[24] Weisbuch C and Lampel G 1972 *Proc. 11th Int. Conf. on the Physics of Semiconductors* (Warsaw: PWN) p 1327
[25] Titkov A N, Safarov V I and Lampel G 1979 *Proc. 14th Int. Conf. on the Physics of Semiconductors (Inst. Phys. Conf. Ser. 43)* ed B L H Wilson (Bristol: Institute of Physics Publishing) p 1031
[26] Kauschke W, Mestres N and Cardona M 1987 *Phys. Rev.* B **35** 3843
[27] Elliot R J 1954 *Phys. Rev.* **96** 266
[28] Yafet Y 1963 *Solid State Physics* vol 14, ed F Seitz and D Turnbull (New York: Academic) p 1
[29] D'yakonov M I and Perel' V I 1971 *Sov. Phys.–JETP* **33** 1053
[30] D'yakonov M I and Perel' V I 1972 *Sov. Phys.–Solid State* **13** 3023
[31] Dymnikov V D, D'yakonov M I and Perel' N I 1976 *Sov. Phys.–JETP* **44** 1252
[32] Bir G L, Aronov A G and Pikus G E 1976 *Sov. Phys.–JETP* **42** 705
[33] Meier F and Zakharchenya B P (ed) 1984 *Optical Orientation (Modern Problems in Condensed Matter Science vol 8)* (Amsterdam: North Holland)
[34] Pikus G E, Marushchak V A and Titkov A N 1988 *Sov. Phys.–Semicond.* **22** 115
[35] Sakharov V I, Titkov A N, Ermakova N G, Komova E M, Mironov I F and Chaikina E I 1981 *Sov. Phys.–Solid State* **23** 1938
[36] Aronov A G, Pikus G E and Titkov A N 1983 *Sov. Phys.–JETP* **57** 680
[37] Marushchak V A, Stepanova M N and Titkov A N 1983 *Sov. Phys.–Solid State* **25** 2035
[38] Chao H-S, Wong K S, Alfano R R, Unlu H and Morkoc H 1988 *J. Soc. Photo-Opt. Instrum. Eng.* **942** 215
[39] Stolz H, Schwarze D, von der Osten W and Weimann G 1989 *Superlatt. Microstruct.* **6** 271
[40] Stark J B, Knox W H and Chemla D S 1990 *Phys. Rev. Lett.* **65** 3033
[41] Freeman M R, Awschalom D D, Hong J M, Chang L L and Ploog K 1990 *Proc. 20th Int. Conf. on the Physics of Semiconductors* ed E M Anastassakis and J D Joannopoulos (Singapore: World Scientific) p 1129
[42] Freeman M R, Awschalom D D and Hong J M 1990 *Appl. Phys. Lett.* **57** 704
[43] Tackeuchi A, Muto S, Inata T and Fujii T 1990 *Appl. Phys. Lett.* **56** 2213
[44] Damen T C, Leo K, Shah J and Cunningham J E 1991 *Appl. Phys. Lett.* **58** 1902
[45] Damen T C, Viña L, Cunningham J E and Shah J 1991 *Phys. Rev. Lett.* **67** 3432
[46] Webb M D, Condiff S T and Steel D G 1991 *Phys. Rev. Lett.* **66** 934
[47] Bar-Ad S and Bar-Joseph I 1992 *Phys. Rev. Lett* **68** 349
[48] Viña L, Damen T C, Cunningham J E, Shah J and Sham L J 1992 *Superlatt. Microstruct.* **12** 379
[49] Roussignol P, Rolland P, Ferreira R, Delalande C, Bastard G, Vinattieri A, Carraresi L, Colocci M and Etienne B 1992 *Surf. Sci.* **267** 360
[50] Vinattieri A, Shah J, Damen T C, Kim D S, Pfeiffer L N and Sham L J 1993 *Solid State Commun.* **88** 189
[51] Dareys B, Marie X, Amand T, Barrau J, Shekun Y, Razdobreev I and Planel R 1993 *Superlatt. Microstruct.* **13** 353
[52] Dareys B, Amand T, Marie X, Baylac B, Barrau J, Brousseau M, Razdobreev I and Dunstan D J 1993 *J. Physique* IV **3** 351
[53] Bar-Joseph I, Bar-Ad S, Carmel O and Levinson Y 1993 *Optical Phenomena in Semiconductor Structures of Reduced Dimension* vol 248, ed D J Lockwood and A Pinczuk (Dordrecht: Kluwer Academic) p 173
[54] Frommer A, Ron A, Cohen E, Kash J A and Pfeiffer L N 1994 *Phys. Rev.* B **50** 11 833
[55] Muñoz L, Pérez E, Viña L and Ploog K 1995 *Phys. Rev.* B **51** 4247
[56] Baylac B, Amand T, Brousseau M, Marie X, Dareys B, Bacquet G, Barrau J and Planel R 1995 *Semicond. Sci. Technol.* **10** 295
[57] Amand T, Marie X, Robart D, Le Jeune P, Brousseau M and Barrau J 1996 *Solid State Commun.* **100** 445
[58] Snoke D W, Rühle W W, Köhler K and Ploog K 1997 *Phys. Rev.* B **55** 13 789
[59] Amand T, Robart D, Marie X, Brousseau M, Le Jeune P and Barrau J 1997 *Phys. Rev.* B **55** 9880
[60] Nickolaus H, Wuensche H-J and Henneberger F 1999 *Phys. Rev. Lett.* **81** 2586
[61] van der Poel W A J A, Severens A L G J, van Kesteren H W and Foxon C T 1989 *Superlatt. Microstruct.* **5** 115
[62] Gotoh H, Ando H, Kamada H and Chavez-Pirson A 1998 *Appl. Phys. Lett.* **72** 1341
[63] Vinattieri A, Shah J, Damen T C, Goossen K W, Pfeiffer L N, Maialle M Z and Sham L J 1993 *Appl. Phys. Lett.* **63** 3164
[64] Filoramo A, Ferreira R, Roussignol P, Planel R and Thierry-Mieg V 1998 *Phys. Rev.* B **58** 4617
[65] Ivchenko E L, Kopev P S, Kochereshko V P, Uraltsev I N and Yakovlev D R 1988 *JETP Lett.* **47** 486
[66] Roussignol P, Rolland P, Ferreira R, Delalande C, Bastard G, Vinattieri A, Martinez-Pastor J, Carraresi L, Colocci M, Palmier J F and Etienne B 1992 *Phys. Rev.* B **46** 7292
[67] Wagner J, Schneider H, Richards D, Fischer A and Ploog K 1993 *Phys. Rev.* B **47** 4786

[68] Ferreira R, Roussignol P, Rolland P, Bastard G, Delalande C, Vinattieri A and Weimann G 1993 *J. Physique Coll.* II **3** C5 175

[69] Martin M D, Pérez E, Viña L, Gravier L, Potemski M, Ploog K and Fisher A 1988 *Physica* E **2** 186

[70] Le Jeune P, Marie X, Amand T, Romstad F, Perez F, Barrau J and Brousseau M 1998 *Phys. Rev.* B **58** 4853

[71] Kuzma N N, Khandelwal P, Barrett S E, Pfeiffer L N and West K W 1998 *Science* **281** 686

[72] D'yakonov M I and Kachorovskii V Y 1986 *Sov. Phys.–Semicond.* **20** 110

[73] Twardowski A and Herman C 1987 *Phys. Rev.* B **35** 8144

[74] Ferreira R and Bastard G 1991 *Phys. Rev.* B **43** 9687

[75] Bastard G and Ferreira R 1992 *Surf. Sci.* **267** 335

[76] Ferreira R and Bastard G 1993 *Europhys. Lett.* **23** 439

[77] Ferreira R and Bastard G 1994 *Solid-State Electron.* **37** 851

[78] German E P and Subashiev A V 1997 *JETP Lett.* **65** 909

[79] Maialle M Z and Degani M H 1997 *Phys. Rev.* B **55** 13 771

[80] Sham L J 1987 *J. Physique Coll.* **48** C5 381

[81] Uenoyama T and Sham L J 1990 *Phys. Rev. Lett.* **64** 3070

[82] Uenoyama T and Sham L J 1990 *Phys. Rev.* B **42** 7114

[83] Sham L J 1993 *J. Phys.: Condens. Matter* **5** 51

[84] Sham L J 1993 *Optical Phenomena in Semiconductor Structures of Reduced Dimension* vol 248, ed D J Lockwood and A Pinczuk (Dordrecht: Kluwer Academic) p 201

[85] Maialle M Z, de Andrade e Silva E A and Sham L J 1993 *Phys. Rev.* B **47** 15 776

[86] Malshukov A G, Chao K A and Willander M 1995 *Phys. Rev.* B **52** 5233

[87] de Andrade e Silva E A and Rocca G C L 1997 *Phys. Rev.* B **56** 9259

[88] Peyghambarian N, Gibbs H M, Jewell J L, Antonetti A, Migus A, Hulin D and Masselink W T 1984 *Phys. Rev. Lett.* **53** 2433

[89] Hulin D, Mysyrowicz A, Antonetti A, Migus A, Masselink W T, Morkoc H, Gibbs H M and Peyghambarian N 1986 *Phys. Rev.* B **33** 4389

[90] Schmitt-Rink S, Chemla D S and Miller D A B 1985 *Phys. Rev.* B **32** 6601

[91] Amand T, Marie X, Baylac B, Dareys B, Barrau J, Brousseau M, Planel R and Dunstan D J 1994 *Phys. Lett.* A **193** 105

[92] Robart D, Amand T, Marie X, Baylac B, Barrau J, Brousseau M and Planel R 1995 *Ann. Phys., Paris, Suppl.* C2 **20** 91

[93] Viña L, Muñoz L, Pérez E, Fernández-Rossier J, Tejedor C and Ploog K 1996 *Phys. Rev.* B **54** 8317

[94] Stark J B, Knox W H and Chemla D S 1992 *Phys. Rev.* B **46** 7919

[95] Fernández-Rossier J and Tejedor C 1996 *Proc. 23rd Int. Conf. on the Physics of Semiconductors* ed M Schaeffler and R Zimmermann (Singapore: World Scientific) p 2463

[96] Fernández-Rossier J, Tejedor C, Muñoz L and Viña L 1996 *Phys. Rev.* B **54** 11 582

[97] Baumberg J J, Crooker S A, Awschalom D D, Samarth N, Luo H and Furdyna J K 1994 *Phys. Rev.* B **50** 7689

[98] Baumberg J J, Awschalom D D, Samarth N, Luo H and Furdyna J K 1994 *Phys. Rev. Lett.* **72** 717

[99] Crooker S A, Baumberg J J, Flack F, Samarth N and Awschalom D D 1996 *Phys. Rev. Lett.* **77** 2814

[100] Crooker S A, Baumberg J J, Flack F, Samarth N and Awschalom D D 1997 *Phys. Rev.* B **56** 7574

[101] Smyth J F, Tulchinsky D A, Awschalom D D, Samarth N, Luo H and Furdyna J K 1993 *Phys. Rev. Lett.* **71** 601

[102] Freeman M R, Awschalom D D, Hong J M and Chang L L 1990 *Phys. Rev. Lett.* **64** 2430

[103] Oestreich T, Schönhammer K and Sham L J 1995 *Phys. Rev. Lett.* **75** 2554

[104] Kikkawa J M, Smorchkova I P, Samarth N and Awschalom D D 1997 *Science* **227** 1284

[105] Kikkawa J M, Smorchkova I P, Samarth N and Awschalom D D 1998 *Physica* E **2** 394

[106] Shah J 1993 *Optical Phenomena in Semiconductor Structures of Reduced Dimension* vol 248, ed D J Lockwood and A Pinczuk (Dordrecht: Kluwer Academic) p 117

[107] Phillips R T 1994 *Coherent Optical Interactions in Semiconductors* (New York: Plenum)

[108] Wang H, Shah J, Damen T C and Pfeiffer L N 1995 *Phys. Rev. Lett.* **74** 3065

[109] Heberle A P, Baumberg J J and Koehler K 1995 *Phys. Rev. Lett.* **75** 2598

[110] Sham L J, Oestreich T and Schönhammer K 1998 *Physica* E **2** 388

[111] Heberle A P, Ruehle W W and Ploog K 1994 *Phys. Rev. Lett.* **72** 3887

[112] Marie X, Le Jeune P, Amand T, Brousseau M, Barrau J, Paillard M and Planel R 1997 *Phys. Rev. Lett.* **79** 3222

[113] Amand T, Marie X, Le Jeune P, Brousseau M, Robart D, Barrau J and Planel R 1997 *Phys. Rev. Lett.* **78** 1355

[114] D'yakonov M I, Marie X, Amand T, Le Jeune P, Robart D, Brousseau M and Barrau J 1997 *Phys. Rev.* B **56** 10 412

[115] Gravier L, Potemski M and Ploog K 1995 *Proc. 22nd Int. Conf. on the Physics of Semiconductors* ed D J Lockwood (Singapore: World Scientific) p 1213

[116] Feldmann J, Peter G, Göbel E O, Dawson P, Moore K, Foxon C T and Elliott R J 1987 *Phys. Rev. Lett.* **59** 2337
[117] Hanamura E 1988 *Phys. Rev.* B **38** 1228
[118] Deveaud B, Clerot F, Roy N, Satzke K, Sermage B and Katzer D S 1991 *Phys. Rev. Lett.* **67** 2355
[119] Andreani L C, Tassone F and Bassani F 1991 *Solid State Commun.* **77** 641
[120] Vinattieri A, Shah J, Damen T C, Kim D S, Pfeiffer L N, Maialle M Z and Sham L J 1994 *Phys. Rev.* B **50** 10 868
[121] Nithisoontorn M 1989 *Phys. Rev. Lett.* **62** 3078
[122] Ekardt W, Losch K and Bimberg D 1979 *Phys. Rev.* B **20** 3303
[123] von Kesteren H W, Cosman E C, Greidanus F J A M, Dawson P, Moore K J and Foxon C T 1988 *Phys. Rev. Lett.* **61** 129
[124] Blackwood E, Snelling M J, Harley R T, Andrews S R and Foxon C T 1994 *Phys. Rev.* B **50** 12 246
[125] Aichmayr G, Jetter M, Viña L, Fernández-Rossier J, Tejedor C, Dickerson J, Camino F and Mendez E E 1999 *March Mtg of the APS (Atlanta, GA)*
[126] Oskotskij B D, Subashiev A V and Mamaev Y A 1997 *Phys. Low-Dim. Struct.* **1+2** 77
[127] Vasil'ev A M, Daiminger F, Straka J, Forchel A, Kochereshko V P, Sandler G L and Uraltsev I N 1993 *Superlatt. Microstruct.* **13** 97
[128] Omori T, Kurihara Y, Takehuchi Y, Yoshioka M, Nakanishi T, Okumi S, Tsubata M, Tawada M, Togawa K, Tanimoto Y, Takahashi C, Paba T and Mizuta M 1994 *Japan. J. Appl. Phys.* **33** 5676
[129] Shah J 1991 *Hot Carriers in Semiconductors Nanostructures: Physics and Applications* (New York: Academic)
[130] Johnson M 1994 *IEEE Spectrum* **12** 47